EMITTANCE MEASUREMENT FOR SPring-8 LINAC USING FOUR SIX-ELECTRODE BPMS

K. Yanagida*, S. Suzuki, H. Hanaki, JASRI/SPring-8, Sayo, Hyogo, Japan

Abstract

We installed four six-electrode beam position monitors at the end of the SPring-8 linear accelerator to measure the emittances and the Twiss parameters. Our method was to measure the second-order relative moments as we changed the magnetic field strengths of four quadrupole magnets, and to deduced the emittances and the Twiss parameters at the reference point. An entire calibration, which included effects up to the fifth-order moments with effective aperture radii, was essential and indispensable for precise measurements.

INTRODUCTION

For Twiss parameter matching of electron beams, emittances were measured at the end of the SPring-8 1-GeV linear accelerator (linac). Wire scanner monitors and profile monitors (PMs) had previously been utilized. However, such destructive monitors are not practical for daily operation because of frequent gain tuning in the case of signal saturation or reduction to the noise level.

In the previous works the emittances or the beam sizes were measured using non-destructive multi-electrode beam position monitors (BPMs) [1] [2]. Fortunately, a wide dynamic range signal processor has been developed in the SPring-8 linac [3], and we started a design study of a six-electrode (6E) BPM [4] for a second-order moment measurement and constructed such a system [5].

In this conference, we present the following four items, including emittance measurements, as the compilation of work related to second-order moment measurements:

- Signal difference composed of up to fifth-order moments.
- Effective aperture radius.
- Entire calibration.
- Emittance measurement by the Q-scan method.

SIGNAL DIFFERENCE FORMULAE

At LINAC2012, we proposed the entire calibration and effective aperture radius concepts [5]. The effective aperture radius was defined as a proportional coefficient between nth-order signal difference C_n (S_n) and absolute moment P_n (Q_n).

This expression was accurate when an electron beam was located within 1 mm of the BPM duct center. On the other hand, the beam positions must exceed 3 mm when the beam was swept for an entire calibration. To ensure measurement accuracy, the signal differences were modified to include more higher-order moments [6].

The signal differences were defined for the SPring-8 linac 6EBPM with circular cross-section [4] as

$$\begin{aligned}
C_1 &= \frac{V_1 - V_3 - V_4 + V_6}{V_1 + V_3 + V_4 + V_6},\\
S_1 &= \frac{V_1 + V_3 - V_4 - V_6}{V_1 + V_3 + V_4 + V_6},\\
C_2 &= \frac{V_1 + V_3 + V_4 + V_6 - 2(V_2 + V_5)}{V_1 + V_3 + V_4 + V_6 + 2(V_2 + V_5)},\\
S_2 &= \frac{V_1 - V_3 + V_4 - V_6}{V_1 + V_3 + V_4 + V_6},\\
S_3 &= \frac{V_1 - V_2 + V_3 - V_4 + V_5 - V_6}{V_1 + V_2 + V_3 + V_4 + V_5 + V_6},
\end{aligned} \tag{1}$$

where V_d ($d = 1, \cdots, 6$) is the output voltage from electrode d (Fig. 1).

C_m and S_m are expressed by nth-order absolute moments P_n and Q_n ($m \leqq n \leqq 5$) with corresponding effective aperture radius $R_{C,SmP,Qn}$ as follows:

$$\begin{aligned}
C_1 &\approx \frac{2P_1}{R_{C1P1}}\left(1 - \frac{2P_2}{R^2_{C1P2}} + \frac{4P_2^2}{R^4_{C1P2}} + \frac{2P_4}{R^4_{C1P4}}\right)\\
&\quad + \frac{2P_3}{R^3_{C1P3}} - \frac{2P_5}{R^5_{C1P5}},\\
S_1 &\approx \frac{2Q_1}{R_{S1Q1}}\left(1 - \frac{2P_2}{R^2_{S1P2}} + \frac{4P_2^2}{R^4_{S1P2}} + \frac{2P_4}{R^4_{S1P4}}\right)\\
&\quad + \frac{2Q_3}{R^3_{S1Q3}} + \frac{2Q_5}{R^5_{S1Q5}},\\
C_2 &\approx \frac{2P_2}{R^2_{C2P2}}\left(1 + \frac{2P_2}{R^2_{C2P2'}}\right) - \frac{2P_4}{R^4_{C2P4}},\\
S_2 &\approx \frac{2Q_2}{R^2_{S2Q2}}\left(1 - \frac{2P_2}{R^2_{S2P2}}\right) + \frac{2Q_4}{R^4_{S2Q4}},\\
S_3 &\approx \frac{2Q_3}{R^3_{S3Q3}}.
\end{aligned} \tag{2}$$

Each $R_{C,SmP,Qn}$ is given in Table 1.

Note that in Eq. 2, C_1 and S_1 include the second-order absolute moment, P_2. This means that C_1 and S_1 are slightly affected by the beam shape because a horizontally (vertically) long beam shape has a positive (negative) second-order relative moment, P_{g2} (Eq. 4).

P_n and Q_n can be expressed by the lengths and the arguments of a two-dimensional polar coordinates: b_G, β_G, a_{gk} and α_{gk} (Eq. 3). b_G and β_G are the components of first-order absolute moments P_1 and Q_1. a_{gk} and α_{gk} are the components of kth-order relative moments P_{gk} and

* ken@spring8.or.jp

ISBN 978-3-95450-142-7

Table 1: Effective aperture radii $R_{C,SmP,Qn}$ [mm]

R_{C1P1}	18.688	R_{S1P2}	23.155	R_{C2P4}	18.029
R_{C1P2}	23.155	R_{S1Q3}	16.570	R_{S2Q2}	17.594
R_{C1P3}	∞	R_{S1P4}	19.953	R_{S2P2}	23.155
R_{C1P4}	19.953	R_{S1Q5}	19.531	R_{S2Q4}	17.392
R_{C1P5}	17.499	R_{C2P2}	18.906	R_{S3Q3}	16.570
R_{S1Q1}	32.368	$R_{C2P2'}$	32.746		

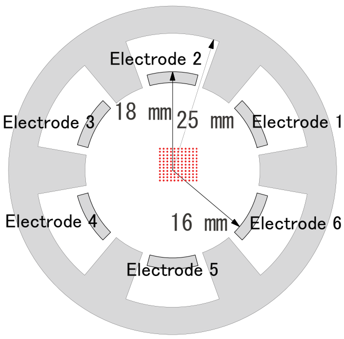

Figure 1: Cross-section of 6EBPM and mapping points (denoted by red circles) in entire calibration.

Q_{gk} [4].

$$P_n = \sum_{k=0}^{n} \frac{n! b_G^{n-k} a_{gk}^k}{k!(n-k)!} \cos\left\{(n-k)\beta_G + k\alpha_{gk}\right\},$$

$$Q_n = \sum_{k=0}^{n} \frac{n! b_G^{n-k} a_{gk}^k}{k!(n-k)!} \sin\left\{(n-k)\beta_G + k\alpha_{gk}\right\}, \quad (3)$$

$$P_{gk} = a_{gk}^k \cos k\alpha_{gk},\ Q_{gk} = a_{gk}^k \sin k\alpha_{gk},$$

$$a_{g1} \equiv 0,\ P_1 = b_G \cos\beta_G,\ Q_1 = b_G \sin\beta_G.$$

Since the SPring-8 linac 6EBPM can detect only three relative moments, P_{g2}, Q_{g2}, and Q_{g3} [5], the other relative moments are neglected or regarded as zero. Then Eq. 3 is re-written:

$$\begin{aligned}
P_2 &= p_{G2} + P_{g2},\ Q_2 = q_{G2} + Q_{g2},\\
P_3 &= p_{G3} + 3b_G a_{g2}^2 \cos(\beta_G + 2\alpha_{g2}),\\
Q_3 &= q_{G3} + 3b_G a_{g2}^2 \sin(\beta_G + 2\alpha_{g2}) + Q_{g3},\\
P_4 &= p_{G4} + 6b_G^2 a_{g2}^2 \cos(2\beta_G + 2\alpha_{g2}), \qquad (4)\\
Q_4 &= q_{G4} + 6b_G^2 a_{g2}^2 \sin(2\beta_G + 2\alpha_{g2}),\\
P_5 &= p_{G5} + 10b_G^3 a_{g2}^2 \cos(3\beta_G + 2\alpha_{g2}),\\
Q_5 &= q_{G5} + 10b_G^3 a_{g2}^2 \sin(3\beta_G + 2\alpha_{g2}),
\end{aligned}$$

where p_{Gk} and q_{Gk} are called the kth-order centroid moments:

$$p_{Gk} = b_G^k \cos k\beta_G,\ q_{Gk} = b_G^k \sin k\beta_G,\ (1 \leqq k). \quad (5)$$

ENTIRE CALIBRATION

The entire calibration method was previously described [5]. The beam position was swept, as shown in Fig. 1.

Typical measured moments are shown in Figs. 2, 3, and 4. As the steering-magnet currents were changed, beam positions P_1 and Q_1 varied (Fig. 2); however, relative moments P_{g2} and Q_{g2} behaved like constants (right sides of Figs. 3 and 4).

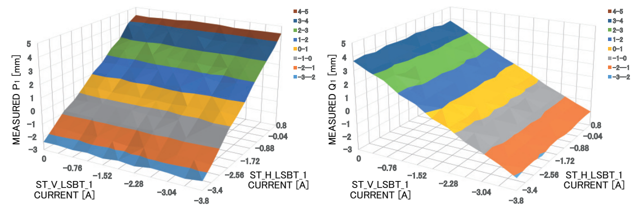

Figure 2: Typical measured P_1 [left] and Q_1 [right].

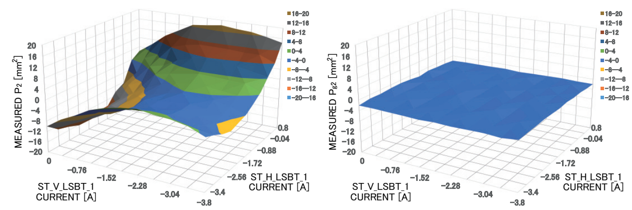

Figure 3: Typical measured P_2 [left] and P_{g2} [right].

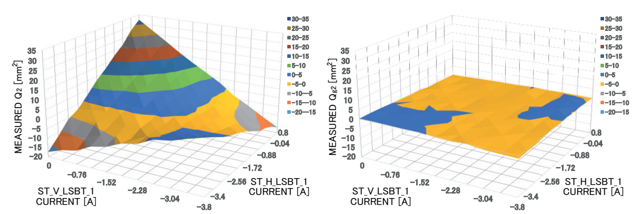

Figure 4: Typical measured Q_2 [left] and Q_{g2} [right].

EMITTANCE MEASUREMENT

An emittance measurement by the Q-scan method was carried out at the end of the linac. There were four 6EBPMs and four quadrupole magnets (QMs) (Fig. 5). Each 6EBPM was placed ~70 mm upstream of each QM.

The QM currents were appropriately changed (Fig. 6). The QM-current sign means that the positive (negative) current corresponds to focusing (defocusing). Measured second-order relative moments P_{g2_M} are shown in Fig. 7. There were eleven measurement sets in this Q-scan.

Our emittance calculation method is described below. We assume trial emittances and Twiss parameters at the location of upstream profile monitor PM_LS_1 and calculate envelopes σ_{H_C} and σ_{V_C} downstream.

The emittances and Twiss parameters were gradually changed to minimize the square of the difference between the measured and calculated second-order relative moment, P_{g2_M} and $P_{g2\_C} = \sigma_{H\_C}^2 - \sigma_{V\_C}^2$ [4].

The deduced emittances and Twiss parameters are summarized in Table 2. Figure 8 shows σ_{H_C}, σ_{V_C}, P_{g2_C}, and P_{g2_M} as the result of the eleventh-measurement set.

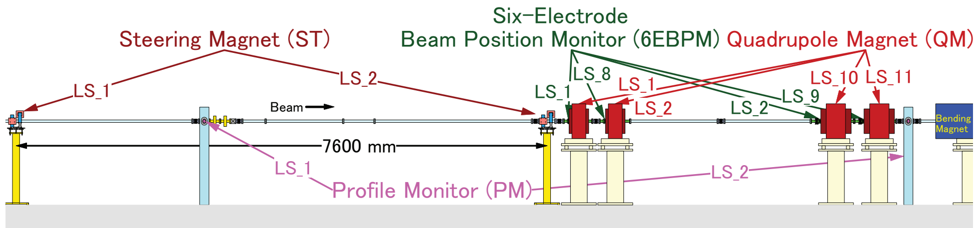

Figure 5: Schematic layout of equipment for emittance measurement.

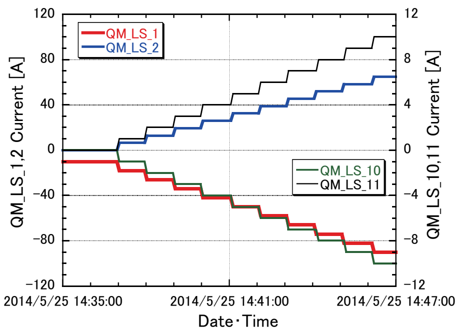

Figure 6: Set QM current in Q-scan.

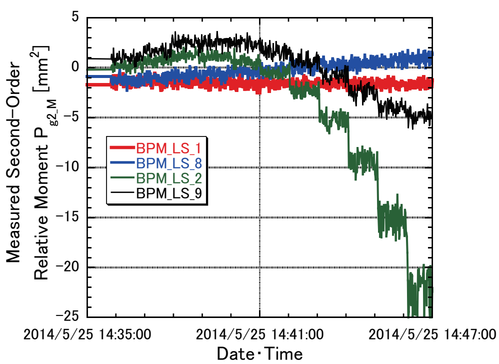

Figure 7: Measured second-order relative moment P_{g2_M}.

In Fig. 8, P_{g2_C} and P_{g2_M} show good agreement, and this result proves the validity of such emittance measurement.

Table 2: Deduced Emittances and Twiss Parameters

Parameter	Horizontal	Vertical
ε [πmm · mrad]	0.168 ± 0.002	0.299 ± 0.001
β [m]	14.7 ± 0.1	5.7 ± 0.2
α	2.25 ± 0.04	0.50 ± 0.03

The beam profiles were measured for verification (Fig. 9). The measured beam sizes, σ_{H_M} and σ_{V_M}, are plotted in Fig. 8 and are comparable to σ_{H_C} and σ_{V_C}.

SUMMARY

We successfully carried out emittance measurement using only 6EBPMs and proved the validity of the Q-scan method. The entire calibration and signal differences composed of up to fifth-order moments were indispensable for precise second-order moment measurements.

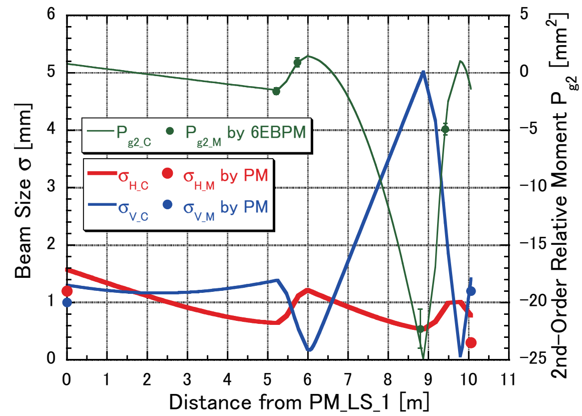

Figure 8: Calculated and measured σ_H, σ_V and P_{g2}.

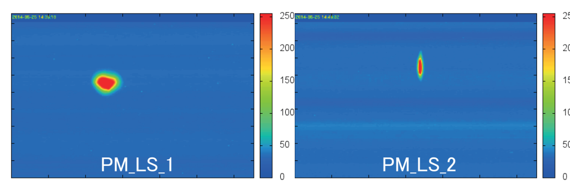

Figure 9: Measured beam profiles (8-bit-processed).

REFERENCES

[1] R. H. Miller, et al., "Nonintercepting Emittance Monitor", Proc. 12th Int. Conf. High-Energy Accel. (HEAC'83), Fermilab USA, 1983, pp. 603-605.

[2] T. Suwada, et al., Phys. Rev. ST Accel. Beams **6**, 032801 (2003), http://journals.aps.org/prstab/pdf/10.1103/PhysRevSTAB.6.032801.

[3] K. Yanagida, et al., "Signal Processor for SPring-8 Linac BPM", Proc. of the 5th European Workshop on Diagnostics and Beam Instr., Grenoble France, May 2001, pp. 162-164, http://accelconf.web.cern.ch/accelconf/d01/papers/PM02.pdf.

[4] K. Yanagida, et al., Phys. Rev. ST Accel. Beams **15**, 012801 (2012), http://link.aps.org/doi/10.1103/PhysRevSTAB.15.012801.

[5] K. Yanagida, et al., "Design and Beam Test of Six-electrode BPMs for Second-order Moment Measurement", Proc. of the 26th Int. Linac Conf., Tel-Aviv Israel, Sept. 2012, pp. 464-466, http://accelconf.web.cern.ch/AccelConf/LINAC2012/papers/tuplb09.pdf.

[6] K. Yanagida, et al., "Third-Order Moment Effect of Beam Position Measurements", Proc. of the 10th Annual Meeting of Particle Accel. Soc. of Japan, Nagoya, August 2013, pp. 197-201, http://www.pasj.jp/web_publish/pasj10/proceedings/PDF/MOOS/MOOS03.pdf

ISBN 978-3-95450-142-7